Valence and core electronic excitations in $KHgC_4$ and $KHgC_8$

M. E Preil
Laboratory for Research on the Structure of Matter and Department of Physics, University of Pennsylvania, Philadelphia, Pennsylvania 19104

L. A. Grunes*
Xerox Webster Research Center, Building 114, Webster, New York 14580

J. J. Ritsko
IBM Thomas J. Watson Research Center, P.O. Box 218, Yorktown Heights, New York 10598

J. E. Fischer
Laboratory for Research on the Structure of Matter and Department of Materials Science and Engineering, University of Pennsylvania, Philadelphia, Pennsylvania 19104

(Received 18 June 1984)

Electron-energy-loss spectroscopy has been used to measure the electronic excitations of the stage-1 and -2 mercurographitides, $KHgC_4$ and $KHgC_8$, respectively. Results for these ternary compounds are compared to similar spectra of the stage-1 and -2 binary intercalation compounds, KC_8 and KC_{24}. Plasmon peaks at 2.1 and 6.7 eV in the stage-1 compound, and 1.6 and 6.7 eV for the stage-2 compound are in good agreement with the optical results. From 1 to 6 eV, the presence of excess oscillator strength in the ternaries compared to the corresponding-stage binary compounds is attributed to interband excitations involving electrons in intercalant-derived bands. The measured Fermi-energy shifts upon intercalation also indicate that the charge transfer from K to graphite is incomplete in the KHg compounds and that some of the original K($4s$) charge is retained in intercalant bands. In the region between 10 and 40 eV, fine structure is observed in the mercurographitide spectra as in the case of KC_8, confirming the earlier assignment of these features to backfolded interband transitions associated with the MC_8 in-plane structure. Comparison of the C($1s$) and K($2p$) core-level excitations with similar data from x-ray photoemission experiments shows that the K($4s$) bands are unoccupied in all four compounds studied here. Based on the above evidence, a model is presented for the charge-transfer mechanism in the ternary compounds. This model is compared with the observed superconducting properties of these compounds, and emphasizes the importance of three-dimensional intercalant-derived bands in the superconductivity of these materials.

INTRODUCTION

Graphite intercalation compounds (GIC's) containing mercury-potassium amalgam have attracted a great deal of attention lately, particularly because of their superconducting properties.[1,2] Both the stage-1 and -2 ternary compounds, $KHgC_4$ and $KHgC_8$, respectively, have been found to exhibit superconductivity,[3] and there have been reports of a stage-3 superconducting compound as well.[4] This is in contrast to the binary compounds, where only the stage-1 KC_8 superconducts, while the stage-2 KC_{24} remains normal down to at least 60 mK.[5] From a rigid-band viewpoint, the large interlayer spacings of the mercurographitides would suggest that the contributions to the electronic properties from the graphite layers should be highly two dimensional. These two observations taken together indicate that the KHg GIC's should make an ideal laboratory for the study of two-dimensional effects in superconducting systems. The possibility even exists for observing a crossover from three- to two-dimensional superconductivity in higher-stage compounds.[4,6] (A similar dimensionality crossover has been reported in the case of pyridine-intercalated transition-metal dichalcogenides.[7]) Studies on the effects of pressure[8,9] and magnetic fields[6,10] on the superconducting transition temperature T_c have already been reported. In order to correctly interpret these results, it is necessary to understand the charge-transfer mechanism involved in the intercalation process. If, for example, the K($4s$) charge was delocalized among the various constituent layers (K, Hg, and C) instead of being transferred completely to the graphite π bands, this would provide electronic coupling in the third dimension. In this case, these materials would still exhibit three-dimensional behavior, even in the limit of large graphite-layer-plane separation. For this reason, it is particularly important to determine how much of the K($4s$) charge is donated to graphitelike states, how much is transferred to Hg-derived states, and how much, if any, is retained in states with potassium s character.

Efforts to determine the electronic structure of these

compounds have so far included optical[11–13] and x-ray photoelectron[12] (XPS) spectroscopic studies of the stage-1 and -2 compounds. The onsets of interband transitions in the optical data, and the C(1*s*) core levels in the XPS work, indicated that approximately the same amount of K(4*s*) charge *per carbon atom* is donated to the graphite bands as in the corresponding binary compounds, KC_8 and KC_{24}. Since there is far more alkali metal per carbon atom in the ternaries, however (twice as much in $KHgC_4$ as in KC_8, 3 times as much in $KHgC_8$ as in KC_{24}), this leaves a significant amount of potassium *s* charge which must either be denoted to Hg-derived bands or retained in potassiumlike states. The implication of the XPS results[12] is that more charge is present in these intercalant states in the stage-2 compound $KHgC_8$ than in the stage-1 $KHgC_4$. This observation is particularly interesting since $KHgC_8$ has the higher T_c of the two, despite the fact that specific-heat measurements[3] indicate a lower density of states at the Fermi level. The XPS results imply that it is not the total density of states that is important in determining T_c, but the density of intercalant, *s*-like states. Similarly, Shubnikov–de Haas measurements[4] show strong evidence for *s*-like intercalant-derived carriers in the stage-2 compound. Further evidence for the importance of three-dimensional states in these GIC's comes from compressibility measurements,[14] which show $KHgC_4$ to be twice as compressible as KC_8. This points to much softer interlayer interactions in the ternary compound relative to the binary one, and indicate that the charge transfer along the *c* axis is more spread out over the various layers. In the terminology of Ref. 14, the *c*-axis charge distribution is more "metallic" (i.e., delocalized) in $KHgC_4$, while KC_8 is more "ionic" (i.e., clearly defined positively and negatively charged layers).

Electron-energy-loss spectroscopy (EELS) has been shown to be a sensitive probe of the electronic properties of intercalated graphite.[15–19] EELS measures the energy-loss function $\mathrm{Im}(-1/\epsilon)$; by performing a Kramers-Kronig (KK) analysis of the energy-loss data, the real and imaginary parts of the complex dielectric function ϵ can be obtained and the elementary excitation spectrum of the system can be determined. In this paper we present EELS spectra for both core and valence electronic excitations of $KHgC_4$ and $KHgc_8$. This study is in agreement with the optical results in the low-energy valence region, and extends our knowledge of the complex dielectric function to 40 eV. The free-electron plasmons occur at the same energies as in the binary compounds, but the plasmon peaks are broadened and damped by low-energy interband transitions. We will show that these transitions involve intercalant-derived energy bands, indicating the importance of the intercalant levels, as well as the graphite π bands, in determining the electronic properties of these compounds. Evidence is presented for excitations from backfolded graphite π bands, as in KC_8, confirming the backfolded origin of these features, consistent with the existence of a 2×2 in-plane superlattice in the ternary compounds. Core-level excitations show that the K(4*s*) states are unoccupied in both $KHgC_4$ and $KHgC_8$, as in KC_8 and KC_{24}, indicating that the excess charge in the mercurographitides which is not transferred to the π bands must be present in states with primarily mercury character.

The following section contains a brief description of the experimental procedures. We then present the electron-energy-loss spectra and discuss the main features of the observed energy-loss functions. A Kramers-Kronig integration of the data is performed, and the ϵ_2 spectra are analyzed in detail. We first discuss the low-energy portions of the spectra (0—10 eV) where intraband plasmons and interband transitions involving states near the Fermi level dominate, and then the higher-energy regions (10—40 eV) where potassium core levels and backfolded excitations are the features of interest. C(1*s*) and K(2*p*) peaks are presented and compared to XPS data, and the positions of the final states for potassium core excitations are determined. Finally, the region between the C(1*s*) and K(2*p*) peaks is studied in detail and compared to spectra for pure graphite, and the final states for carbon core-level transitions are found. The paper closes with a summary of our results, and the implications of these findings in understanding the electronic properties of the ternary intercalation compounds is discussed.

EXPERIMENTAL DETAILS

Thin flakes (<1000 Å thick) were cleaved from larger pieces of highly oriented pyrolytic graphite provided by A. Moore of Union Carbide Corporation. The flakes were placed on copper electron-microscope grids and intercalated using the standard preparation techniques.[20] Samples were characterized by their well-known colors, pink for $KHgC_4$ and blue for $KHgC_8$. Bulk samples prepared in the same intercalation reactions as the flakes were also studied by (00*l*) x-ray diffraction, and showed the correct patterns, indicating that the samples were fully intercalated. Transmission-electron-energy-loss spectra were recorded for 80-keV incident electrons at zero- or finite-momentum transfer parallel to the graphite planes, with an energy resolution of 0.1 eV full width at half maximum (FWHM) and a momentum resolution of 0.05 Å^{-1}. The samples did not show any bulk decomposition within the measurement period of approximately 24 h in the spectrometer vacuum of 2×10^{-8} Torr. This is in contrast to the surface decomposition at room temperature seen in XPS.[12,21] Count rates for these experiments were considerably lower than in previous work,[15–18] due to the large *c*-axis expansion upon intercalation, resulting in thick samples. In addition, the high atomic number *Z* of mercury resulted in a large amount of elastic scattering, leaving less beam available for inelastic scattering. The lower count rate was not a problem for the valence-band region, but did prevent the use of derivative techniques to enhance the core-level spectra.[16]

RESULTS AND DISCUSSION

Figure 1 presents our results for the energy-loss function from 0 to 40 eV at $q=0.1$ Å^{-1} for $KHgC_4$ and $KHgC_8$, compared to the corresponding stage-1 and -2 binary intercalation compounds KC_8 and KC_{24}, respectively. Similar data for potassium metal and pure

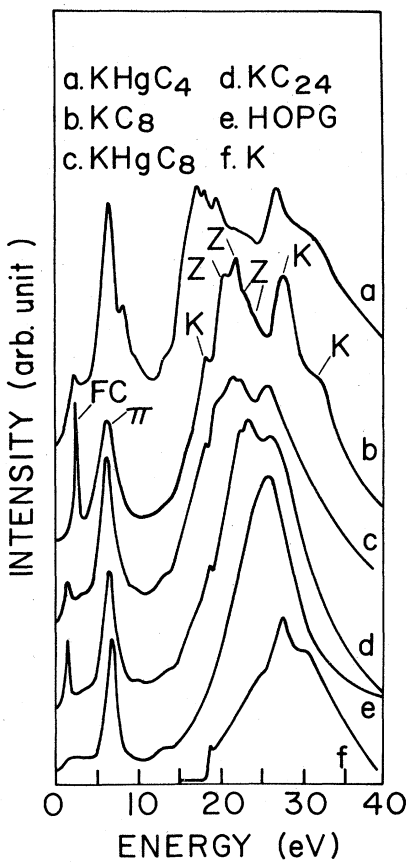

FIG. 1. Energy-loss functions of $KHgC_4$, KC_8, $KHgC_8$, KC_{24}, graphite, and potassium metal at $q=0.1$ Å^{-1} from 0 to 40 eV.

graphite are also shown. First appearances are deceptive; the energy-loss spectra for the stage-1 compounds seem dras- tically different from each other, while the stage-2 compounds look quite similar. It will be seen in the ϵ_2 spectra that these apparently major variations are actually due to very slight differences in the dielectric functions.

Several important features can be seen in the energy-loss spectra; these are marked on the curve for KC_8, but appear in the spectra for the other compounds as well. The lowest-energy peak is the free-carrier plasmon ("FC" in the figure) which represents the collective oscillation of the free conduction electrons. Located between 6 and 7 eV is the π interband plasmon; the peak here corresponds to the exhaustion of the oscillator strength for $\pi\rightarrow\pi^*$ transitions. Taft and Philipp[22] showed that this interband plasmon should actually occur closer to 12.5 eV, but screening effects due to the σ electrons shift this feature to lower energy. From 19 to 25 eV the large peak is the $\pi+\sigma$ all-valence electron plasmon. The fine structure marked "Z" represents transitions from zone-folded graphite π bands, while the peaks labeled "K" correspond to potassium core-level excitations.[15] (Note the peaks at approximately the same energies in the potassium-metal spectrum.) The small shoulder at 13 eV is due to a local maximum in the joint density of states for transitions involving σ bands.[16]

In order to discuss the detailed quantitative differences between the compounds under consideration, we must first perform a KK analysis to obtain the complex dielectric function. This is because the energy-loss function $\mathrm{Im}(-1/\epsilon)$ is equal to $\epsilon_2/(\epsilon_1^2+\epsilon_2^2)$, and is therefore sensitive to changes in both the real and imaginary parts of ϵ. This is particularly true when ϵ_1 and ϵ_2 are both small, as is the case above 10 eV. A clear picture of the electronic excitations can thus be seen only after performing the Kramers-Kronig analysis. A correction factor for multiple scattering must be taken into account before performing the KK integration.[17] This factor is practically zero for the very thin binary samples, but becomes appreciable for the thicker ternary compounds. All data shown here have been corrected for multiple scattering. The $\mathrm{Im}(-1/\epsilon)$ spectra are normalized so as to satisfy the oscillator-strength sum rule,[17,23] and also to give $\mathrm{Re}(1/\epsilon)=0$ at zero energy.[17] The results of this analysis are shown in Fig. 2 from 0 to 10 eV, and in Fig. 3 from 10 to 40 eV. We will concentrate first on the low-energy region, where EELS and optical-reflectivity data can be compared.

The best way to check the validity of the KK analysis of the energy-loss data is to compute the optical-reflectivity spectrum from the Kramers-Kronig–derived dielectric function and compare it to accurate optical measurements. Figure 4 shows our calculated normal-incidence reflectivity spectra compared to the measured spectra of Ref. 12. The match between the calculated and measured data is quite good, confirming both the accuracy of the KK analysis and the proper staging of the samples. The most noticeable discrepancy occurs at the plasma-edge minima, which occur at the same energies in the optical and EELS data, but have slightly different magnitudes. Such minor discrepancies are expected since the energy-loss data are taken at 0.1 Å^{-1}, while the optical data correspond to $q=0$. (It is difficult to determine the dielectric function from $q=0$ energy-loss data because of the strong energy dependence of the scattering cross section as $q\rightarrow 0$.[23])

The low-energy EELS valence-band spectra (Fig. 1) agree with the results of the earlier optical study.[12] The

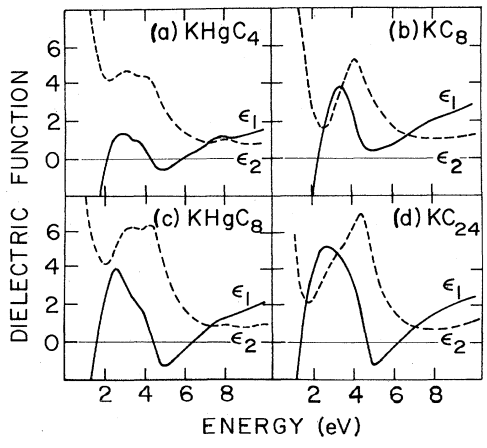

FIG. 2. Real and imaginary parts of the dielectric function for the stage-1 and -2 ternary and binary compounds from 0 to 10 eV.

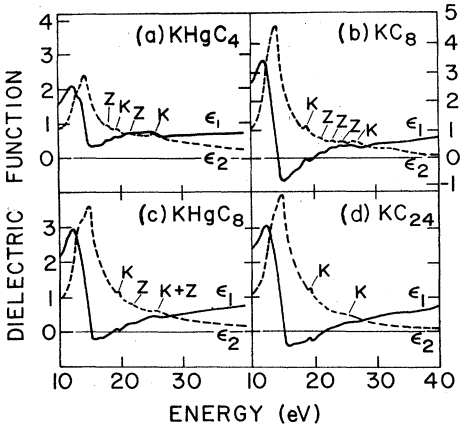

FIG. 3. Real and imaginary parts of the dielectric function for the stage-1 and -2 ternary and binary compounds from 10 to 40 eV.

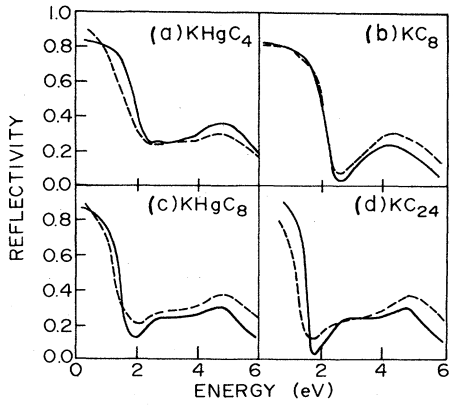

FIG. 4. Normal-incidence reflectivity functions. Dashed curves are as calculated from the energy-loss data; solid curves are measured reflectivity spectra of Preil and Fischer (Ref. 12).

screened free-electron plasmon peaks occur at the same energies in the ternary compounds as in their binary counterparts, although the ternary peaks are strongly damped by low-energy interband transitions which begin at about 1 eV. The imaginary part of the dielectric function can be broken down into free-electron and interband components. The free-electron term decreases with increasing energy according to the simple Drude expression, while the interband term starts to contribute at a threshold energy E_T equal to twice ΔE_F, the shift in the Fermi level upon intercalation.[24] Using this method, we find $\Delta E_F = 1.35$, 1.2, 0.85, and 0.85 (± 0.15) eV for KC_8, $KHgC_4$, KC_{24}, and $KHgC_8$, respectively, in good agreement with the optical results.[12,13] The ϵ_2 spectra for the mercurographitides also show a second, lower-energy threshold at 1.2 eV in $KHgC_4$ and at 1.1 eV in $KHgC_8$. This threshold is incompatible with graphite $\pi \rightarrow \pi^*$ transitions since it would imply a very small shift in the Fermi level. Instead, the second threshold has been ascribed to transitions involving intercalant-derived bands, probably Hg,[11,12] since they are unique to the ternary compounds. It is the presence of these additional low-energy excitations below the plasma frequency which damps the plasmon peaks in the loss function, as noted above. Assuming a rigid-band model for the graphite π bands, the Fermi-level shift is directly correlated with the amount of charge transferred to the graphite bands. The fact that the Fermi-level shifts are the same in the ternaries as in the corresponding binaries indicates that roughly the same total amount of charge is donated to the graphite bands in $KHgC_4$ as in KC_8, and in $KHgC_8$ as in KC_{24}. Since there is more K($4s$) charge per carbon atom in the ternaries, however, a sizable fraction of the original $4s$ charge must either be transferred to Hg-derived bands or retained in potassiumlike states.

At higher energy (Fig. 2) all four compounds show a peak in the loss function between 6 and 7 eV, which corresponds to the interband peak in ϵ_2 seen at 4.0 eV for the stage-1 and 4.3 eV for the stage-2 compounds. A similar peak is found at 4.3 eV in pure graphite, and is associated with the $\pi \rightarrow \pi^*$ interband plasmon. The strength of the peak in ϵ_2 decreases monotonically from graphite through KC_{24}, KC_8, $KHgC_8$ to $KHgC_4$, corresponding to the increasing interplanar separation d and the resulting decrease in oscillator strength per unit volume. This decrease is partially offset by the addition of charge to the graphite π bands in the intercalation process. Since the integral of ϵ_2 multiplied by the energy must equal the number of electrons in the occupied bands,[23] the addition of charge to the π bands is equivalent to increasing the number of oscillators per unit volume. These new oscillators will show up in the intraband (free-carrier) contribution to ϵ_2. Assuming the potassium is fully ionized in the binaries, and that the same amount of charge per carbon atom is donated to the graphite bands in the ternaries as in the binaries, we can estimate the expected oscillator strength for $\pi \rightarrow \pi^*$ transitions in all four compounds compared to pure graphite. These estimates are shown in Table I, and are compared to the observed ratio of in-

TABLE I. Oscillator strengths in intercalation compounds compared to graphite.

Compound	Average c-layer spacing (Å)	Fraction of graphite value	Charge per carbon atom[a]	Expected strength relative to graphite[b]	Observed strength relative to graphite
KC_8	5.35	0.62	1.125	0.70	0.66
KC_{24}	4.35	0.77	1.042	0.80	0.78
$KHgC_4$	10.15	0.33	1.125	0.37	0.75
$KHgC_8$	6.75	0.50	1.042	0.52	0.96
Graphite	3.35	1.00	1.000	1.00	1.0

[a]Defined as one π electron plus $1/n$ transferred electrons per carbon atom, where $n = 8$ for stage-1 and 24 for stage-2 compounds.

[b]Product of columns 2 and 3.

tegrated oscillator strength for the GIC's relative to the value in graphite. This simple approach explains the binary data reasonably well. For the ternaries, however, there is almost twice as much oscillator strength in the peak than predicted from the simple model. This discrepancy is not due to our assumptions concerning the charge transfer in the mercurographitides. Even if one assumed complete charge transfer from K to C levels in the KHg GIC's (which is incompatible with the earlier discussion), the sum rules on ϵ_2 would still be far greater than predicted. In short, graphitic transitions alone are insufficient to account for the observed oscillator strength in the ternary compounds. The clear implication is that part of the oscillator strength is due not to the graphite π bands, but to intercalant-derived transitions which underlie the graphitic excitations.

Referring back to Fig. 1, the energy-loss spectrum of $KHgC_4$ shows two features for which no explanation currently exists; a shoulder at about 5.5 eV, and a sharp peak at 8.35 eV. There is a slight shoulder at 8.5 eV in $KHgC_8$ as well. These features were reproduced in several samples prepared at different times. Mercury has a $5d$ doublet at 7.6 and 9.8 eV which is clearly seen in XPS, both in mercury metal[25] and in the intercalation compounds.[12] The 8.35-eV peak could represent a transition from the lower $5d$ state to a final state 0.75 eV above E_F. Such a final state is in reasonable agreement with the optical data, which showed intercalant-derived interband transitions starting at just over 1 eV. If this were the case, we should expect to see a peak at about 11 eV in EELS corresponding to transitions from the higher-energy $5d$ state to the same final state above E_F. No such peak is seen, although it is possible that it is unobservable owing to the strong onset of graphite $\sigma \rightarrow \sigma^*$ transitions in this energy range.

Turning to the higher-energy part of the valence-band spectra (10—40 eV), we can see that despite the marked difference in the general appearance of the energy-loss functions for the stage-1 compounds (Fig. 1), the shapes of the ϵ_2 spectra are quite similar (Fig. 3). KC_8 shows five distinct peaks in ϵ_2 in this energy region, at 18.9, 21.3, 22.9, 24.3, and 27.7 eV. The larger peaks at 18.9 and 27.7 eV were identified by Ritsko *et al.*[15] as potassium excitations, as can be seen by looking at the energy-loss function of K metal. The remaining three peaks were shown to be due to graphite π bands folded back into the smaller Brillouin zone imposed by the potassium in-plane superlattice. In a later paper, Grunes *et al.*[16] demonstrated that only the 2×2 structure associated with MC_8 compounds (M =K, Rb, and Cs) gives rise to observable features due to backfolded excitations; the $\sqrt{3}\times\sqrt{3}$ superlattice of LiC_6 gives an essentially featureless ϵ_2 spectrum in this energy range. This is because the transitions observed in compounds with 2×2 in-plane structure involve initial $2p$ (π) states at the Γ point of the original graphite Brillouin zone and final $3p$ (π) states at Q. The 2×2 superlattice folds the Q point back to Γ, resulting in a set of strongly allowed interband transitions with a high joint density of states. The $\sqrt{3}\times\sqrt{3}$ structure, on the other hand, folds the Q point back on itself. The interband transitions are thus forbidden, and a structureless energy-loss spectrum is predicted (and observed) in this energy region for MC_6 compounds. Ritsko *et al.*[15] also showed that careful analysis of the energy spacings and relative amplitudes of the backfolded features in ϵ_2 are highly sensitive to the strengths of both the in-plane modulation potential V_{intra} and the interplane modulation potential V_{inter}. Thus these authors were able to arrive at quantitative estimates for the strength and anisotropy of the graphite-to-metal s-band interaction in KC_8. The very slight features seen in ϵ_2 of KC_{24} were explained as being due either to a small amount of stage-1 material in the stage-2 sample, or to small commensurate islands of potassium where the local in-plane structure resembles KC_8.

With this background we can understand the features seen in the ϵ_2 spectra of both $KHgC_4$ and $KHgC_8$ (Fig. 3). As in the case of the binary compounds, the large peak near 14 eV is due to σ interband transitions. This peak in ϵ_2 gives rise to the sharp drop in ϵ_1 and the resulting $\pi+\sigma$ interband plasmon in the energy-loss function. The fact that the $KHgC_4$ energy-loss function appears to be so different from that of KC_8, while ϵ_2 looks so similar, is now seen to be due to the fact that ϵ_1 does not pass through zero for $KHgC_4$ as it does for the other compounds. This, in turn, is due to a combination of the higher background of interband transitions, and the way in which the Kramers-Kronig relations cause ϵ_1 to be scaled with changes in ϵ_2. The values of ϵ_2 for $KHgC_4$ are much smaller than for KC_8 because of the reduced oscillator strength per unit volume. This not only reduces the overall values of ϵ_1, but also introduces a small positive baseline which keeps ϵ_1 from passing through zero at the σ interband plasmon. The two potassium peaks seen in KC_8 at 18.9 and 27.7 eV are also seen in the other spectra at similar energies.

Both $KHgC_4$ and $KHgC_8$ have the same 2×2 potassium in-plane superlattice as KC_8,[20] and so the same type of backfolding effects should be evident. These zone-folding effects are clearly indicated by the peaks in ϵ_2 at 18.1 and 22 eV in $KHgC_4$, and at 21.7 and 22.0 eV in $KHgC_8$ (Fig. 3). In addition, the peak at 26 eV in $KHgC_4$, which is attributed to potassium $3p$ excitations, is much larger relative to the $3p$ onset at 19.6 eV than in any of the other compounds, suggesting that part of the amplitude in this peak may also be due to backfolded excitations. It is tempting to compare the energies and amplitudes of these zone-folded features in the mercurographitides to the three corresponding peaks in KC_8, which appear as weak modulations in ϵ_2 at 21.3, 22.9, and 24.3 eV. As noted above, the KC_8 spectrum is well described by Ritsko *et al.*[15] in terms of a simple tight-binding calculation. Unfortunately, the KC_8 calculation cannot simply be extended to cover the case of the ternary compounds. Ritsko's model depended on the equivalence of the three Q points of the Brillouin zone. For the ternary compounds, however, the presence of the mercury layer breaks the symmetry by selecting one particular sublattice for occupation by Hg atoms. Thus, instead of a 6×6 Hamiltonian coupling the six degenerate $3p_z$ bands, as in KC_8, we should expect the bands at one of the three Q points to be split off from the other bands, resulting in a new set of allowed transitions. The problem is further complicated

TABLE II. XPS and EELS core-level excitation energies. All values in eV, ±0.2 eV.

	XPS[a]		EELS		
	C(1s)	K(2p)	C(1s)	K(2p)	Δ[b]
$KHgC_4$	285.00	293.55	284.65	295.60	2.40
$KHgC_8$	284.90	293.45	284.80	296.00	2.65
KC_8	284.95	294.30	284.65	296.40	2.40
KC_{24}	285.05	294.95	284.70	296.50	1.90

[a]From Ref. 11.
[b]Defined in text, Eq. (1).

by the possibility of K-Hg interactions, in addition to the potassium-graphite coupling (see below and Ref. 14). Finally, because some of the states at the Fermi level in the mercurographitides are intercalant derived, and not purely graphitic as in KC_8,[18,26] the possibility exists for extensive hybridization of the graphite bands with the intercalant bands. Thus, a simple rigid-band model considering only graphite π bands the graphite-potassium interaction is far from adequate as a description of the backfolded excitations in $KHgC_4$ and $KHgC_8$. We can safely conclude that the features seen in this study do arise from transitions involving backfolded π bands because of their similarity to the features seen in KC_8; a more exact assignment of which bands are involved must await detailed band-structure calculations.

We turn now to the C(1s) and K(2p) core levels, shown in Fig. 5 for all four compounds at $q=0$ Å^{-1}. Table II summarizes the positions of the graphite and potassium core levels as measured by EELS and XPS.[12] No mercury core levels could be seen in EELS due to the low cross sections for electron excitation from the heavy Hg atoms.[27] The XPS peak energies correspond to transitions from the respective core levels to the vacuum (measured with reference to E_F), while the EELS peaks represent transitions to unoccupied states in the vicinity of the excited atom. The EELS peaks are strongly modified by the electron-hole interaction so that the measurement actually reveals the density of final conduction-electron states in the presence of the core hole. Mele and Ritsko[17] showed that the electron-hole interaction does not alter the bandwidth of the conduction-electron states nor shift the onset or endpoint of the spectrum. Its main effect is to enhance the oscillator strength in the region just above the threshold at the expense of the higher-energy excitations. The result is that the excitation probability to the lowest empty state is magnified, and thus the onset of the core energy-loss peaks is a good indicator of band minima or the Fermi-level cutoff. For this reason the data given in Table II for EELS are the threshold values. The very sharp onsets of the C(1s) peaks make it clear that the carbon core-level energy loss indicates transitions to the unoccupied states at the Fermi energy. This is consistent with the rigid-band model of intercalation in which E_F moves through the graphite π bands, so that there are always π states at the Fermi level of the intercalation compounds.

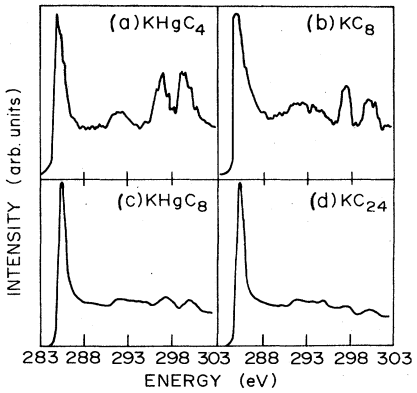

FIG. 5. C(1s) and K(2p) core-level excitation spectra of the stage-1 and -2 ternary and binary compounds at 0.0 Å^{-1} from 283 to 303 eV.

As shown in Fig. 5, no such sharp onsets for the K(2p) peaks are observed, so that the final states involved in these transitions must be above E_F. By comparing XPS and EELS, we can determine how far above the Fermi level these final states are. The XPS levels tell us the binding energies of the initial states; the EELS thresholds give the transition energies from these initial states to the final states. The difference Δ between the two measured quantities gives us the energy of this final state above E_F. The selection rules which govern the electron-energy-loss process require the final state for K(2p) transitions to be a potassiumlike conduction band with either s or d character. If the metal s band retains some charge, then the final state for EELS transitions would be at the Fermi level, and must equal zero. If, on the other hand, the K(4s) band is unoccupied, then the final state for the K(2p) excitations must be above E_F. In this case, Δ is the energy of the lowest potassium-derived conduction-band state above the Fermi level. The fact that the C(1s) threshold clearly marks the Fermi level should compensate for any screening differences between the two experiments. As in Ref. 16, this energy Δ is given by

$$\Delta = E([\mathrm{C}(1s)\text{-}\mathrm{K}(2p)]_{\mathrm{XPS}}) - E([\mathrm{C}(1s)\text{-}\mathrm{K}(2p)]_{\mathrm{EELS}}) . \quad (1)$$

(A more detailed description of this procedure is given in Ref. 18.) As seen in Table II, Δ=2.4, 2.65, 2.0, and 1.9 (±0.4) eV for $KHgC_4$, $KHgC_8$, KC_8, and KC_{24}, respectively.

The following question then arises: What is the final state between 2 and 3 eV above E_F in all four compounds? For KC_8, Ritsko and Brucker[18] identified this as the unoccupied K(4s) band, in good agreement with the band structure of DiVincenzo and Rabbi,[28] but in conflict with

the band structures of Inoshita *et al.*[29] and Ohno *et al.*,[30] who showed the K(4*s*) band intersecting the Fermi level (i.e., $\Delta=0$). A peak at the same energy was seen in partial-photoyield spectroscopy,[31] but was attributed to K(2*p*)-K(3*d*) transitions. Since theoretical[32] and experimental[33] results indicate that the K(3*d*) bands are approximately 8 eV above E_F in potassium metal, it is hard to imagine these bands being downshifted by close to 6 eV upon intercalation, while at the same time the 4*s* bands are being shifted up by 1 eV or more. We therefore concur with the assignment of Ritsko and Brucker of these peaks to K(2*p*)-K(4*s*) transitions.

The finding that the K(4*s*) level is above E_F in both $KHgC_4$ and $KHgC_8$ raises the question of what happens to the excess charge which is not transferred to the graphite π bands. The present work supports the idea that the excess K(4*s*) charge is transferred to Hg-derived bands. This agrees with Hérold's hypothesis[20] that, by analogy to $FeCl_3$ intercalation compounds, which can be thought of in terms of an alternating charged layer arrangement (C^+-Cl^--Fe^+-Cl^--C^+), the KHg compounds should have a converse charge sequence (C^--K^+-Hg^--K^+-C^-). It is also possible that some of the K- and Hg-derived levels could form hybridized bands which are spatially delocalized over the K-Hg-K sandwich, while the original K(4*s*) level is moved up in energy. Such hybridization could, for example, involve the potassium 4*p* and mercury 6*s* and 6*p* levels. This effect might be expected since the normally spherical 4*s* wave function would have to develop a node to avoid overlapping the nearby mercury atoms. This node, in turn, would increase the kinetic energy of the 4*s*-derived state. A hybridized state with spatial extent covering both K and Hg layers would not contain this extra kinetic-energy term due to charge confinement, and could therefore fall below the 4*s* level.

Regardless of whether the excess K(4*s*) charge is transferred to mercury-derived bands, or hybridized mercury-potassium bands, it is clear that there must be substantial mercury character at the Fermi level. Optical transitions with mercury bands as either the initial or final states should then be expected to occur at low energies, providing an explanation for the interband transitions involving intercalant levels noted above in the valence-band spectra. Transitions from the K(2*p*) core to this intercalant band at E_F (K-Hg hybrid or Hg derived) would be very weak, since the charge concentration would be centered on the mercury atoms.

The presence of K(4*s*)-derived charge on the mercury sites could also explain the shift to lower binding energy of the XPS potassium core levels in the ternary compounds relative to the binaries (Table II). Owing to the proximity of the mercury atoms to the potassium sites, the initial-state binding energies of the K(2*p*) levels would be reduced by Coulomb repulsion. The fact that this upward shift is greater for the stage-2 compound than the stage-1 compound seems to indicate that there is more charge near the K atoms in $KHgC_8$ than in $KHgC_4$. This is consistent with our previous assignment of the amount of charge transferred from potassium to graphite bands as being the same *per carbon atom* in the ternaries as in the binaries. Since there is twice as much available 4*s* charge in $KHgC_4$ as compared to KC_8, but 3 times as much in $KHgC_8$ compared to KC_{24}, this would mean that about half the original 4*s* charge is retained by K or Hg bands in $KHgC_4$, while two-thirds is retained by these bands in $KHgC_8$. The marked shift of the K(2*p*) levels to lower binding energies in the stage-2 compound supports this hypothesis. This finding could explain the fact that T_c is higher for $KHgC_8$ than for $KHgC_4$, despite the larger total density of states at E_F of the latter. It has been suggested[34–36] that superconductivity in GIC's depends on the existence of *s*-like electrons, and that the coupling between intercalate *s* and graphite π electrons gives rise to the superconducting transition. Thus, although $KHgC_4$ has a higher total density of states at E_F, $KHgC_8$, with more charge in the intercalant-derived bands, has a higher density of *s*-like states, and hence a higher T_c.

Finally, we wish to call attention to the small features seen in the energy-loss spectra of all four compounds (Fig. 5) between the C(1*s*) and K(2*p*) core-level peaks. Figure 6 shows the same energy region for pure graphite at several values of *q* ranging from 0.0 to 0.3 Å^{-1}. Three peaks clearly appear, representing transitions from the C(1*s*) core level to states above the Fermi energy. These peaks are at 6.4, 7.2, and 9.2 eV, in good agreement with the single peak seen at 7 eV by Leapman *et al.*[37] in a recent study with lower energy resolution, and with the two peaks seen at 6.4 and 7.4 eV found by Kincaid *et al.*[38]. The growth of the 7-eV peak with increasing *q* parallel to the *c* axis was studied in detail by Leapman, who concluded that the main C(1*s*) peak corresponds to transitions to π states at E_F, while the higher-energy structure represents transitions to the σ antibonding states above E_F. The peaks which appear at 6.4 and 9.2 eV in our graphite spectrum are seen at the same energies relative to the main peak in all four intercalation compounds, within the experimental accuracy of ± 0.2 eV. In a rigid-band model, as the Fermi level moves upon intercalation (by 0.85 eV for the stage-2 compounds and 1.25—1.35 eV for the stage-1 compounds), the σ antibonding states should remain fixed in energy relative to the other graphite bands. Thus we would expect the σ peaks in the carbon core-level spectrum to move closer to the π peak by an amount ΔE_F. This is not what we observe. (Similar non-

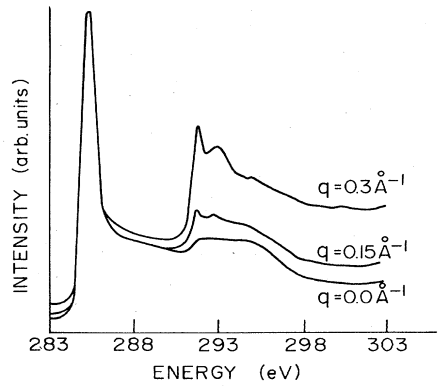

FIG. 6. C(1*s*) core-level excitation spectra of graphite at various momentum transfers from 283 to 303 eV.

rigid effects involving graphite σ bands have been observed in LiC_6 in both angle-resolved[39] and inverse photoemission.[40]) It is clear, however, from the marked similarity of these peaks in graphite and the intercalation compounds, that these are graphitic, and not intercalant-derived, transitions. A full understanding of these features will require calculations of the densities of states of graphite and the intercalation compounds in the presence of the C($1s$) core hole.[17]

SUMMARY

In conclusion, EELS spectra of $KHgC_4$ and $KHgC_8$ confirm the picture of the electronic structure of these compounds found in earlier optical (Refs. 11—13) and XPS (Ref. 12) studies. The valence-band spectra show comparable Fermi-level shifts for the ternaries as well as for their corresponding binary compounds, KC_8 and KC_{24}, implying similar values of charge transfer *per carbon atom* as well. The excess interband oscillator strength found in ϵ_2 results from transitions involving the intercalant levels, which retain the K($4s$) charge that is not donated to the π bands. Features in ϵ_2 between 20 and 25 eV correspond to transitions involving graphite π bands backfolded into the smaller Brillouin zone imposed by the 2×2 in-plane potassium superlattice. The separation of the K($2p$) core levels from the C($1s$) level shows that the potassium $4s$-derived band is unoccupied in both $KHgC_4$ and $KHgC_8$, lying 2.4 and 2.65 (±0.4) eV above E_F for the respective compounds. Thus, the $4s$ charge which is not transferred to the graphite π bands must reside in either Hg-derived bands or hybridized K-Hg levels which fall below the $4s$ band.

ACKNOWLEDGMENTS

We wish to thank I. P. Gates for his help in acquiring the data, H. Mertwoy for assistance in sample preparation, and T. Koch for preparing the figures. This work profited from many helpful discussions with E. J. Mele. Work at the University of Pennsylvania was supported by the National Science Foundation Materials Research Laboratory Program under Grant No. DMR-82-16718.

---

*Present address: Tektronix, Inc., P.O. Box 500, Beaverton, OR 97077.

[1]Proceedings of the Third International Conference on Intercalation Compounds of Graphite, Pont-a-Mousson, France [Synth. Met. **7-8** (1983)].

[2]*Intercalated Graphite,* Vol. 20 of *Materials Research Society Symposium Proceedings,* edited by M. S. Dresselhaus, G. Dresselhaus, J. E. Fischer, and M. J. Moran (North-Holland, New York, 1983).

[3]M. G. Alexander, D. Goshorn, D. Guerard, P. Lagrange, M. El Makrini, and D. Onn, Solid State Commun. **38**, 103 (1981).

[4]G. Timp, B. S. Elman, M. S. Dresslhaus, and P. Tedrow, in *Intercalated Graphite,* Ref. 2, p. 201.

[5]M. Kobayashi and I. Tsujikawa, J. Phys. Soc. Jpn. **50**, 3245 (1981).

[6]Y. Iye and S. Tanuma, Phys. Rev. B **25**, 4583 (1982).

[7]M. Ikebe and Y. Muto, Synth. Met. **5**, 229 (1983).

[8]L. E. DeLong, P. C. Eklund, V. Tondiglio, S. E. Lambert, and M. B. Maple, Phys. Rev. B **26**, 6315 (1982); L. E. DeLong and P. C. Eklund, Synth. Met. **5**, 291 (1983).

[9]Y. Iye and S. Tanuma, Synth. Met. **5**, 257 (1983).

[10]L. A. Pendrys, R. A. Wachnik, F. L. Vogel, P. Lagrange, G. Furdin, M. El Makrini, and A. Hérold, Solid State Commun. **38**, 677 (1981).

[11]M. E Preil, J. E. Fischer, and P. Lagrange, Solid State Commun. **44**, 357 (1983).

[12]M. E Preil and J. E. Fischer, Synth. Met. **8**, 149 (1983).

[13]R. E. Heinz and P. C. Eklund, in *Intercalated Graphite,* Ref. 2, p. 81.

[14]H. J. Kim, H. Mertwoy, T. Koch, J. E. Fischer, D. B. McWhan, and J. D. Axe, Phys. Rev. B **29**, 5947 (1984).

[15]J. J. Ritsko, E. J. Mele, and I. P. Gates, Phys. Rev. B **24**, 6114 (1981).

[16]L. A. Grunes, I. P. Gates, J. J. Ritsko, E. J. Mele, D. P. DiVincenzo, M. E Preil, and J. E. Fischer, Phys. Rev. B **28**, 6681 (1983).

[17]E. J. Mele and J. J. Ritsko, Phys. Rev. Lett. **43**, 68 (1979).

[18]J. J. Ritsko and C. F. Brucker, Solid State Commun. **44**, 889 (1982).

[19]J. J. Ritsko, Phys. Rev. B **25**, 6452 (1982).

[20]A. Hérold, D. Billaud, D. Geurard, P. Lagrange, and M. El Makrini, Physica **105B**, 253 (1981).

[21]M. E Preil, J. E. Fischer, S. B. DiCenzo, and G. K. Wertheim, Phys. Rev. B **30**, 3536 (1984).

[22]E. A. Taft and H. R. Philipp, Phys. Rev. **138**, A197 (1965).

[23]J. Daniels, C. V. Festenberg, H. Raether, and K. Zeppenfeld, in *Optical Constants of Solids by Electron Spectroscopy,* Vol. 54 of *Springer Tracts in Modern Physics,* edited by G. Hohler (Springer, Berlin, 1970), p. 77.

[24]N. H. Hau, J. Blinowski, C. Rigaux, R. LeToullec, G. Furdin, A. Hérold, and R. Vangelisti, Synth. Met. **3**, 99 (1981).

[25]S. Svensson, N. Mårtensson, E. Basilier, P. A. Malmqvist, U. Gelius, and K. Siegbahn, J. Electron. Spectrosc. Relat. Phenom. **9**, 51 (1976).

[26]M. E Preil and J. E. Fischer, Phys. Rev. Lett. **52**, 1141 (1984).

[27]S. E. Schnatterly, in *Solid State Physics,* edited by H. Ehrenreich, F. Seitz, and D. Turnbull (Academic, New York, 1979), Vol. 34, p. 275.

[28]D. P. DiVincenzo and S. Rabii, Phys. Rev. B **25**, 4110 (1982).

[29]T. Inoshita, N. Nakao, and H. Kamimura, J. Phys. Soc. Jpn. **43**, 1237 (1977); **45**, 689 (1978).

[30]T. Ohno, N. Nakao, and H. Kamimura, J. Phys. Soc. Jpn. **47**, 1125 (1979).

[31]C. F. Hague, G. Indelkofer, U. M. Gubler, P. Oelhafen, H.-J. Guntherodt, and J. Schmidt-May, Solid State Commun. **48**, 1 (1983).

[32]F. S. Ham, Phys. Rev. **128**, 82 (1962).

[33]U. S. Whang, E. T. Arakawa, and T. A. Callcott, Phys. Rev. B **6**, 2109 (1972).

[34]Y. Takada, J. Phys. Soc. Jpn. **51**, 63 (1982).

[35]A. Shimizu and H. Kamimura, Synth. Met. **5**, 301 (1983).

[36]R. Al-Jishi, Phys. Rev. B **28**, 112 (1983).

[37]R. D. Leapman, P. L. Fejes, and J. Silcox, Phys. Rev. B **28**, 2361 (1983).
[38]B. M. Kincaid, A. E. Meixner, and P. M. Platzman, Phys. Rev. Lett. **40**, 1296 (1978).
[39]W. Eberhardt, I. T. McGovern, E. W. Plummer, and J. E. Fischer, Phys. Rev. Lett. **44**, 200 (1980).
[40]Th. Fauster, F. J. Himpsel, J. E. Fischer, and E. W. Plummer, Phys. Rev. Lett. **51**, 430 (1983).